Transparent light-emitting electrochemical cells with acid treated multi-wall carbon nanotubes as a top electrode

E.V. Bodiago[a], D.S. Gets[a*], D. R. Ryabov[a], L. E. Zelenkov[a], S. V. Makarov[a,b,c], A. A. Zakhidov[a,d]

[a] *ITMO University, Department of Nanophotonics and Metamaterials, 191002, Russia, Saint Petersburg, Lomonosov str 9*

[b] *Harbin Engineering University, Harbin 150001, Heilongjiang, China*

[c] *Qingdao Innovation and Development Center of Harbin Engineering University, Qingdao 266000, Shandong, China*

[d] *Physics Department, Alan G. MacDiarmid NanoTech Institute, University of Texas at Dallas, Richardson, TX 75083, USA*

**Corresponding author. Tel: +7 951 658-32-96. E-mail: dmitry.gets@metalab.ifmo.ru (Dmitry Gets)*

Keywords: carbon nanotubes, halide perovskites, light-emitting electrochemical cells, semitransparent, acid treatment

Abstract

Halide perovskite light-emitting electrochemical cells (LEC) are color-tunable, efficient, simple, and low-cost single-layer devices, which can be designed in semitransparent architectures for various lightening and display. However, development of highly transparent and conductive electrodes for these devices is a challenging task, requiring not only optimization of the electrode material parameters, but also stable performance without chemical reactions at interfaces. Here we employ multi-walled carbon nanotubes with substantially improved optical and transport properties after their additional chemical processing for efficient semitransparent perovskite LEC. In particular, we develop single-layer perovskite-based LECs with transparency up to 60%, brightness up to 1625 cd/m^2 and maximum current efficiency 3.6 cd/A. We believe that our low-cost and efficient devices would be suitable for semitransparent display technologies.

1. Introduction

Semitransparent light-emitting devices (LED) can be used in various areas, such as head-up displays, augmented reality glasses, car windshields and many others [1]. The first semitransparent display was based on OLED [2] with transparency up to 70 %, but with efficiency around 0.1%, paving the way to development of this new direction involving new materials and designs [3, 4]. In turn, light-emitting electrochemical cell (LEC) have a number of advantages compared to the OLED technology. One of the most important features is the single-layer architecture, which leads to their simple and low-cost fabrication [5, 6]. Moreover, halide perovskites possessing relatively high both electron and ion mobilities have become one of the best materials for LEC [7]. Indeed the unique electrical and optical properties of $CsPbX_3$ perovskites (where X = Cl^-, Br^-, I^-, or their mixtures), make it possible to create LEC, with spectrally narrow and widely tunable emission, which is promising for displays with high color rendering index and broadband color range [8].

There are a number of transparent materials used for electrodes in transparent LED (Table 1) [9], but not all of them (e.g., metals) are suitable for direct contact with a halide perovskite due to corrosive chemical reaction with halogens [10]. More chemically inert material class is conductive oxides (e.g. ITO, FTO, AZO, etc.), but their deposition is a high-temperature process, which is not suitable for a top electrodes [11]. The next class is metal films or metal nanowires, like a silver nanowire network embedded in a polyurethane optical adhesive with transparency at the level 80% [12, 13]. In the case of thin metal films, the transparency of electrode is controlled by the thickness of the layers [14]. The drawback of such metal-based transparent electrodes is the trade-off between transparency and conductivity, for transparent metal films their thickness should less than 20 nm, but it results in significant decrease of the conductivity [15].

One more class is carbon-based materials like carbon nanotubes (CNT) with a transparency exceeding 80% [16], which can potentially solve the problem of device stability in the single layer perovskite LEC and demonstrate excellent optical and electrical characteristics. The internal structure of CNT is hollow, and the surface consists of one or several graphene sheets, which are called single-walled carbon nanotubes (SWCNT) and multi-walled carbon nanotubes (MWCNT), respectively. MWCNT has lower electric and optical parameters compared to SWCNT due to built-in structural defects and an indefinite diameter, which is difficult to control during their synthesis. This, however, makes SWCNT much more expensive than MWCNT [17].

MWCNT was successfully used as an electrode in multilayer OLED, as a transparent anode (T = 60%) [18]. Later, perovskite LEC was developed with vertically oriented MWCNT

as electrodes, where spectral purity of the emitted light was high at low temperatures (23 – 40 K) only [19]. A cathode based on several layers of MWCNT was also reported with perovskite LEC, but the device was nontransparent and had modest parameters: brightness 530 cd/m^2 and current efficiency 0.3 cd/A [20].

In our work, we employ a single layer of MWCNT as a cathode in semitransparent perovskite LEC (see design in Fig. 1a) and propose a method for MWCNT chemical processing by nitric acid to improve their parameters to overcome the limitations inherent for MWCNT. This approach allows us to demonstrate excellent LEC performance with overall transparency up to 60 %, brightness 1625 cd/m^2 (Fig. 1d), and current efficiency 3.6 cd/A (see Supplementary material), which makes them competitive with the devices based on standard materials for electrodes (see Table 1). The various types of transparent electrode materials are summarized in the Table 1 with indications of the parameters of the devices in which they have been applied. One can clearly see that the proposed in this work device with MWCNT as an top electrode exhibit better performance then device with SWCNT both in a single layer structure and MWCNT in the OLED structure. This fact indicates the importance of the proposed pre-treatment of MWCNT.

Table 1. Comparison of various transparent electrode materials used in transparent LED.

Material class		**Electrode material transparency, %**	**External quantum efficiency (%) or current efficiency (cd/A)**	**Architecture of the device**	**Overall device transparency, %**	**Ref.**
Conductive oxides, ITO		90	5.7 %	perovskite LED	55	[21]
Thin metal films		60	10 %	LED based on perovskite nanocrystals	56	[14]
Metal nanowire		80	no information	LEC based inorganic transition metal complexes	no information	[12]
Carbon	SWCNT	90	2.2 cd/A	LEC based on polymer	70	[16]

material	MWCNT	60	2.5 cd/A	OLED	no information	[18]
	MWCNT	60	3.6 cd/A	perovskite LEC	56	this work

2. Results and discussion

Regarding the architecture of our devices, we choose such semitransparent LEC, where the emission layer is perovskite-polymer composition with the addition of lithium salts sandwiched between two electrodes, ITO and MWCNT respectively (Fig. 1a). The band diagram of device is shown on the Figure 1b. All layers in this architecture are transparent, therefore it is possible to obtain a LEC with a transparency up to 60% (Fig. 1e). However, each layer requires its own optimization for better device parameters, which we describe below.

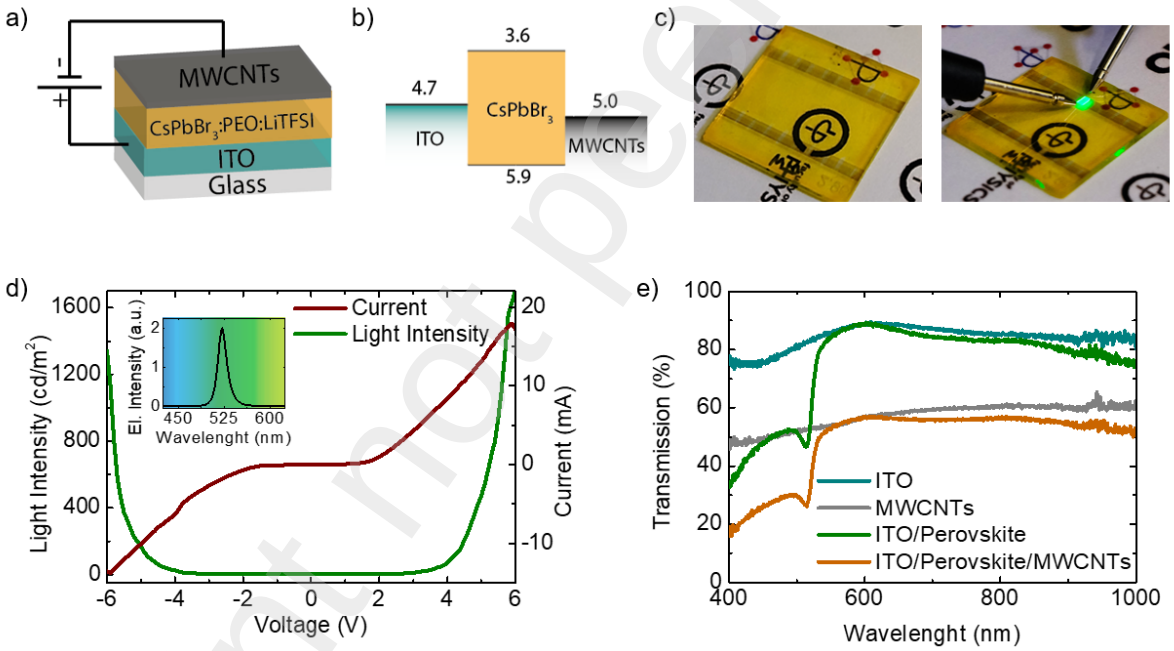

Fig. 1. (a) Illustration of LEC architecture (ITO/CsPbBr3:PEO:LiTFSI/MWCNT). (b) The device band diagram. (c) photos of the devices without (left) and with (right) electroluminescence. (d) current-voltage curve (brown line, right axis), electroluminescence intensity dependence on applied voltage (green line, left axis). Inset: electroluminescence spectrum. (f) Transmission spectra of the device and its various layers.

2.1 Emission layer

A luminescent component in the emissive layer in our devices is perovskite bromide ($CsPbBr_3$), which has better stability than most of the other halide perovskites, because of its

all-inorganic composition [22]. Polyethylene oxide (PEO) is a medium that provides ionic conductivity and lithium salts (LiTFSI) for the formation of a p-i-n structure.

The parameter for assessing the quality of an emissive layer (e.g. defects concentration) is the quantum yield of photoluminescence (PLQY). The PLQY is defined as the ratio of the number of photons emitted to the number of photons absorbed and shows the number of free electron-hole pairs recombined through bimolecular recombination rather than through the defects. As the number of defects increases, the rate of nonradiative recombination via the Shockley-Read-Hall mechanism [23] also increases and the value of PLQY decreases. Therefore, we aim to optimize the PLQY value implying low defects concentration to achieve high brightness of our devices [27, 28].

The analysis of PEO passivation was conducted basing on the measured dependence of PLQY for the $CsPbBr_3$:PEO films with different ratios between perovskite and polymer. We observe that PLQY grows with increase of the PEO amount (Fig. 2a). It is well known that PEO passivates different defects in the perovskite thin film, such as defects in the crystal structure (e.g. halogen vacancy) and, also, the increase of the polymer amount can lead to the better morphology of the whole thin film [29, 30]. However, the increase in the amount of polymer leads to higher resistance of the perovskite-polymer layer (Fig. 2a). Thus, the most optimal ratio between perovskite and polymer is 1:0.2.

There are two factors affecting the PLQY value with increase of the annealing temperature (Fig. 2b) [28]. Firstly, $CsPbBr_3$ has three different phases: an orthorhombic phase at room temperature, a tetragonal phase at temperatures above 88°C, and a cubic phase at temperatures above 130°C [29]. When the temperature crosses the phase transition point, the lattice structure is getting distorted and large stresses occur inside the crystal, which can lead to a higher concentration of vacancies and defects affecting the luminescent properties of the material. Secondly, the melting point of PEO is 66-75°C [30], and, therefore, at the higher temperature the polymer melts and does not cover the surface of perovskite grains. As a result, there is no passivation of defects at higher temperature, and, thus, our perovskite thin films have the most optimal quality at low-temperature annealing.

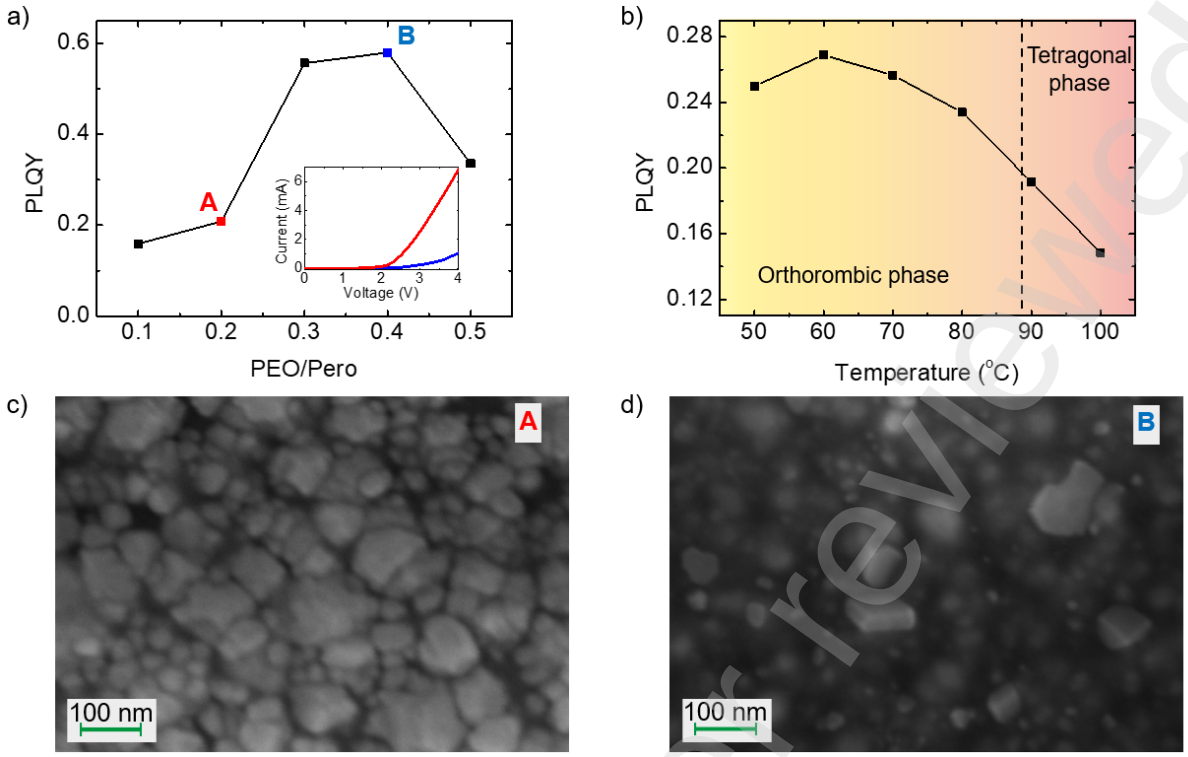

Fig. 2. Dependencies of PLQY of thin films on ratio between perovskite and polymer (a) and on annealing temperatures (b). (c) and (d) SEM images for 1:0.2 and 1:0.4 PEO:$CsPbBr_3$ ratios, respectively.

2.2 Influence of acid vapors on resistance of MWCNT

MWCNT was synthesized by the catalytic chemical vapor phase method [31]. After the synthesis, CNT has undesirable contamination such as amorphous carbon, carbon nanoparticles, residual catalyst, and other graphite impurities that lead to lower properties, for many applications, CNT requires additional chemical treatment for improving properties [32 – 34]. There are various chemical methods for purification and functionalization of CNT, the most widely used is oxidative purification: exposure to ozone, treatment by H_2O_2, oxygen plasma, and acid treatment [35, 36, 38]. There are several types of acid treatment using HNO_3: treatment with boiling HNO_3, treatment with a concentrated mixture of H_2SO_4/HNO_3 in an ultrasonic bath, and treatment by the acid vapor [37, 39, 40].

To study the change in electrical properties of MWCNT, we investigated the change in resistance of MWCNT during the processing by the acid treatment. Treatment of MWCNT with the acid vapor leads to decrease in resistance, which indicates the purification of MWCNT. In the case of nitric acid, the resistance changes by 60%, whereas in the case of other acids, the change in resistance is 30% or less (Fig. 3a).

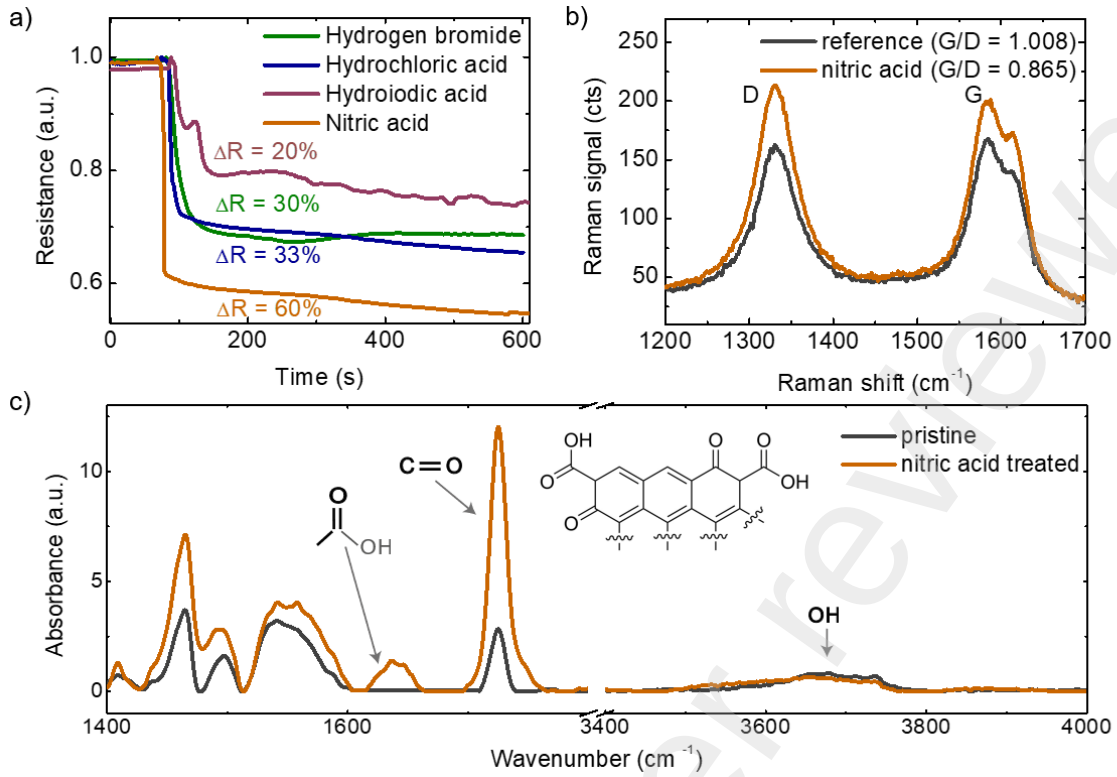

Fig. 3. (a) Influence of acid vapors on resistance (R) of MWCNT. (b) Raman spectra of MWCNT before (black line) and after (orange line) acid treatment. (c) FTIR spectra of MWCNT before (black line) and after (orange line) acid treatment.

The oxidation process of the MWCNT surface corresponds to breaking of chemical bonds in the graphene lattice and appearance of functional groups at the sites of broken chemical bonds. The study of the number of defects in the tube structure was carried out by Raman spectroscopy. The Raman spectra of MWCNT have two peaks: the D-band at 1340 cm^{-1} corresponds to disordered structural bonds, defects or amorphous carbon, and the G-band around 1600 cm^{-1} corresponds to the presence of crystalline carbon, whereas the I_G/I_D ratio describes the quality of MWCNT [38]. The smaller this ratio, the lower the quality of MWCNT. As seen from the Raman spectra in Fig. 3b, some defects are formed on the surface of MWCNT during the acid treatment. However, the treatment with nitric acid vapor can lead to the removal of amorphous carbon and various impurities in the sample, which can form oxygen-containing groups, resulting in the D-band intensity growth.

To understand what types of groups are formed, Fourier-transform infrared spectroscopy (FTIR) of MWCNT was carried out (Fig. 3c). The FTIR spectra show the presence of oxygen-containing groups such as carbonyl group (C=O) and carboxyl group (COOH) after modification with the nitric acid vapor. MWCNT untreated with nitric acid vapor exhibit very low peaks around 3640 cm^{-1} and 1728 cm^{-1} at the FTIR spectra corresponding to

OH and C=O bonds, respectively. The OH peak is associated with the observed water molecules in MWCNT, whereas the peak at 1728 cm^{-1} is associated with the frequency of C=O vibrations, which indicates the presence of carbonyl groups formed during the synthesis. After acid treatment with nitric acid vapor, the additional peak at 1650 cm^{-1} appears in the FTIR spectra, corresponding to the formation of carboxyl groups (COOH) [39].

2.3 Densification of MWCNT

After deposition of MWCNT on a substrate, the important step is their densification for electrical contact with the emission layer. The densification process can be carried out using either the dry [40] or liquid [41] methods. In the former case, a CNT layer is deposited at low pressure, and later, when returning to atmospheric pressure. A pressure difference is established between the outer and inner sides of the deposited thin film, which causes the thin film to deform inherently, and, consequently, the CNT is compressed, forming a compacted bundle. In the latter case, different liquids are used: ethanol or acetone [42, 43], acids [44], and others. But all of them are not suitable in the case of a perovskite-polymer composite, since they easily dissolve the formed thin film.

The densification process should not affect the film morphology of the emissive layer. Therefore, it is important that the densificator does not dissolve PEO and perovskite. According to the literature data [45], a list of antisolvents was formed (see Supplementary material), and we studied their effect on film morphology. As seen from the data presented, isopropyl alcohol (IPA) increasingly changes the morphology of the film and PLQY value changes from 15% to 2%. In comparison, diisopropyl ether (DIPE) does not make any changes in the thin film, and the PLQY value is preserved. As a result, DIPE is more suitable for densification of MWCNT on top of the perovskite-polymer composite.

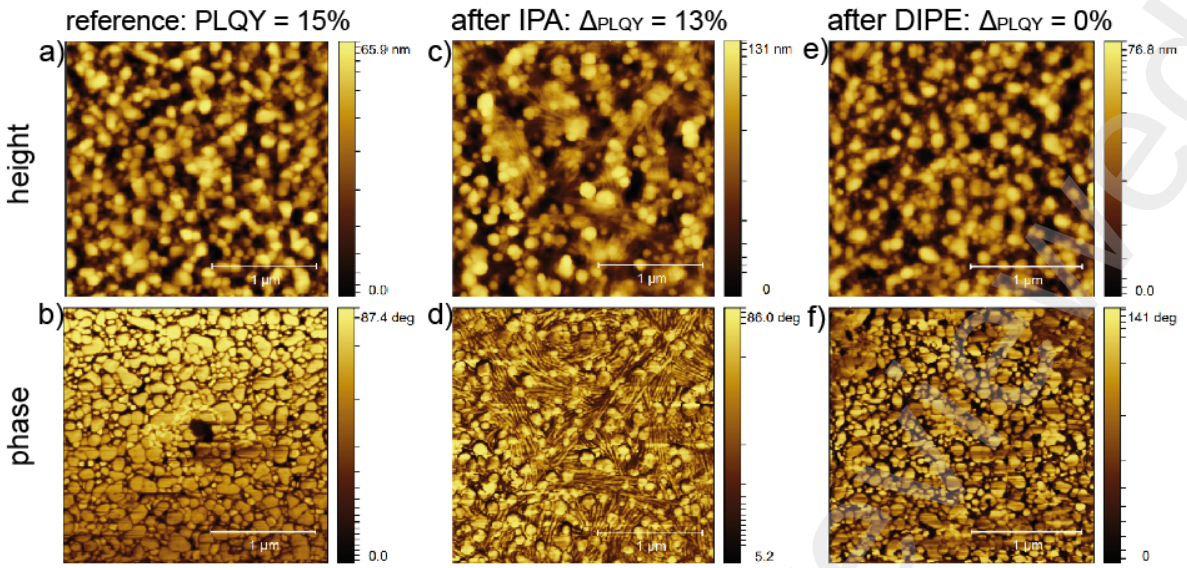

Fig. 4. AFM height profiles for pristine sample (a) and after treatment by IPA (c) and DIPE (e). AFM phase profiles for pristine sample (b) and after treatment by IPA (d) and DIPE (f) of perovskite-polymer composite.

2.4 Perovskite LEC with MWCNT.

The architecture of the studied devices has the architecture of a single-layer electrochemical cell with two transparent electrodes: ITO as a bottom electrode and MWCNT as a top electrode. The emission layer is a composition of bromine perovskite ($CsPbBr_3$) mixed with an electrolyte consisting of lithium salts (LiTFSI) and a polyethylene oxide.

An important feature of LEC is that the electrical parameters are less dependent on the work function of the electrodes, which is due to the operation principle of LEC. Operation principle of LEC based on ion migration and form the p-i-n structure within the emission layer [46]. When voltage is applied, mobile ions of perovskite and lithium salts in the active layer drift towards the interfaces of the electrodes and form the electrical double layers at the interfaces. The electric fields created at the interfaces improve injection conditions of charge carriers, which recombine while moving into the bulk of the active layer. So, the perovskite LEC shows visible electroluminescence when applied voltage higher than V_{th} = 2.4 V (Fig. 5a).

The use of MWCNT treated by the acid vapor as an electrode makes it possible to improve the characteristics of the device (Fig. 5a,c,d) since the structure of the MWCNT changes, conductivity becomes better, and functional groups improve the adhesive properties [47]. But with increasing time and temperature of the acid treatment of MWCNT, the device

parameters such as current, brightness and efficiency become worse again, and the shunt resistance increases owing to MWCNT oxidation.

Capacitance–voltage (CV) measurements were carried out to determine the number of defects (Fig. 5b). The analysis of CV characteristics can qualitatively show the behavior of charge carriers. There are four regions on the CV curve. The first region corresponds to low applied voltages, and the injected charge carriers can be neglected, therefore the device capacitance will be defined as geometrical capacitance, i.e. as a constant. In the second region, the applied voltage is still small and injected charge carriers cannot overcome the energy barrier, so they are accumulated at the interface between the two materials, and the capacitance increases. In the third region, the voltage becomes sufficient to overcome the energy barrier by charge carriers, leading to diffusion and transport of charge carriers, and, thus, this is a diffusion capacitance. In the fourth region, the applied voltage is the turn-on voltage of the device, where injection and recombination of charge carriers take place. For devices with a high injection barrier due to defects at the interface, charge carriers will be accumulated at the interface and the peak capacitance will be higher. In the case of a low injection barrier, there will be no accumulation of charge carriers, and the capacitance in the fourth region will decay faster [48]. So, the acid treatment for five minutes allows to remove existing defects, but it is not sufficient for the formation of functional groups on the surface, which leads to an improvement in the adhesive properties of MWCNT. Further, the number of defects increases, which in this case are carboxyl groups. At the same time, an increase in processing time does not allow keeping the device parameters high. Fifteen minutes is the optimum time for the acid treatment of the MWCNT. Further processing increases the formation of functional groups, which leads to a low electrical properties of the MWCNT, similarly to graphene and graphene oxide. When graphene is oxidized, resistance will increase very strongly, which will lead to the formation of dielectric graphene oxide [49].

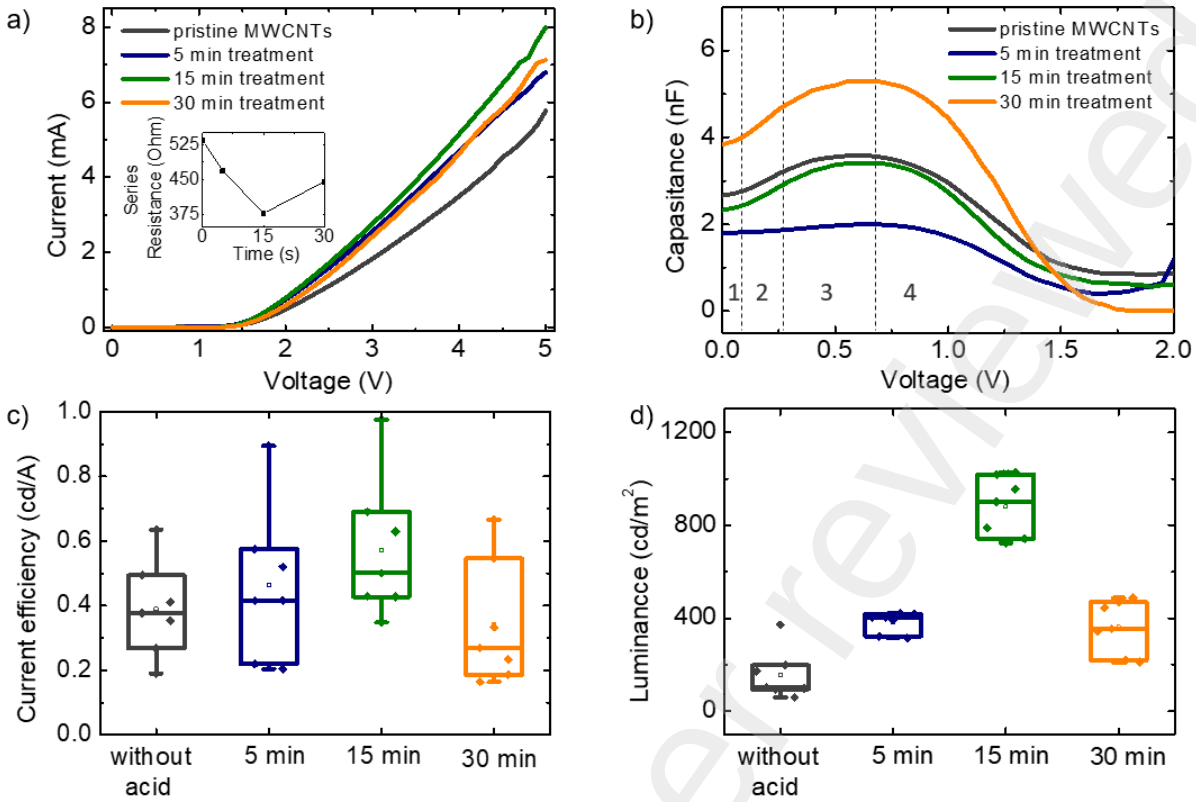

Fig. 5. (a) Current-voltage curves of the developed LEC. Inset: acid treatment time dependence of series resistance. (b) Capacitance-voltage curves for the device with different time of acid treatment of MWCNT. Device statistic for current efficiency (c) and luminance (d) at 5 V.

3. Material and methods

3.1 Solution preparation

A $CsPbBr_3$ solution was prepared by dissolving $PbBr_2$ and CsBr with a molarity of 0.2 in an anhydrous DMSO solution. A PEO solution was prepared by dissolving 20 mg PEO (M_w = 1 000 000 g/mol) in 1 ml DMSO, then the solution was stirred overnight at 60°C at 300 rpm. The perovskite-polymer solution $CsPbBr_3$:PEO (1:0.2 by weight) by mixing required masses of PEO and $CsPbBr_3$. Next, the perovskite-polymer solution required an amount of 2% LiTFSI solution DMSO (10mg/ml). The resulting solution was stirred for 1 hour at 300 rpm.

3.2 Perovskite film deposition

LEC devices (Fig. 1a) were fabricated on a transparent, indium-tin oxide (ITO) coated glass substrate, deposition of perovskite-polymer composite was conducted in a glovebox with nitrogen atmosphere. Before the deposition of the emission layer, the substrates were cleaned from various kinds of contaminants, after which they were subjected to thermal treatment and treatment in oxygen plasma for 10 minutes at 40 W. The cleansing consists of several stages.

Each substrate was sequentially cleaned with a detergent solution, followed by a NaOH solution, deionized water, acetone, and isopropyl alcohol in an ultrasonication bath for 5 minutes. To obtain an emission layer with a thickness of 160 nm, precursor solutions were spin-coated onto ITO substrates at 1000 rpm for 1 min and then vacuum and thermally annealed at 60 °C for one and five minutes respectively. The film morphology was controlled by AFM spectroscopy (Fig. 4).

3.3 MWCNT deposition

MWCNT fiber was used as a top electrode. MWCNT fiber was used as a top electrode. The method of treating MWCNT with acid was taken from our previous work [50]. Before deposition, MWCNTs were thermally treated at 250 ℃ next they were subjected to nitric acid vapor treatment at 70 ℃. The densification of MWCNT on perovskite-polymer film was done by Diisopropyl ether, after that the devices were vacuum dried for one hour to remove residual solvent from the surface.

3.4 Measurement setups

The current-voltage (IV) curves were measured with Keithley 2400 sourcemeter. The electroluminescence measurements were carried out in parallel with the measurements of the IV curves using spectroradiometer Instrument Systems CAS 120.

Measurements of PLQY were carried out using an integrating sphere Labsphere, an excitation laser with wavelength 405 nm, two wheels with ND filters (FW212CNEB) and QE Pro spectrometer. Measurement procedure was carried out with accordance with article de Mello [51].

The experimental Raman scattering spectra were obtained using HORIBA LabRam HR spectrometer and confocal optical microscopy setup with 1800 mm^{-1} diffraction grating. The sample was excited with 632.8 nm HeNe continuous-wave laser radiation focused through an optical microscope objective (50×, NA = 0.55). Laser power excitation was adjusted by increase of spot diameter to prevent the damage of the MWCNT [52].

The measurement of FTIR spectra was carried out using a IR-Fourier spectrometer Nicolet 8700 with a spectral range of 11000 - 350 cm^{-1}.

4. Summary

We have shown that chemical treatment of the MWCNT improves their electrical properties, allowing them to be used as electrodes in devices. The use of functionalized MWCNT allows the fabrication of semitransparent perovskite LEC with total transparency

56%, brightness 1625 cd/m^2, and current efficiency 3.6 cd/A. Acid treatment of MWCNT has an optimal time, when defects are passivated and MWCNT has better electrical properties. According to our comparative analysis in Table 1, our devices have demonstrated the best current efficiency at high level of transparency among the reported semitransparent LEC or OLED. Therefore, we believe that the developed low-cost and efficient approach would be suitable for semitransparent display technologies.

Declaration of competing interest

The authors declare that they have no known competing financial interests or personal relationships that could have appeared to influence the work reported in this paper.

Acknowledgements

This work was supported by the Russian Science Foundation (project № 19-73-30023).

The FTIR measurements were supported by St. Petersburg State University (project No 93021679)

References

[1] Y. Huang, E. Hsiang, M. Deng, and S. Wu, "Mini-LED , Micro-LED and OLED displays : present status and future perspectives," *Light: Science & Applications*, 2020.

[2] G. Gu, V. Bulović, P. E. Burrows, S. R. Forrest, and M. E. Thompson, "Transparent organic light emitting devices," *Applied Physics Letters*, vol. 68, no. 19, pp. 2606–2608, 1996.

[3] K. H. Kim *et al.*, "Crystal Organic Light-Emitting Diodes with Perfectly Oriented Non-Doped Pt-Based Emitting Layer," *Advanced Materials*, vol. 28, no. 13, pp. 2526–2532, 2016.

[4] M. G. Song *et al.*, "Highly reliable and transparent Al doped Ag cathode fabricated using thermal evaporation for transparent OLED applications," *Organic Electronics*, vol. 76, no. August 2019, p. 105418, 2020.

[5] F. Yan and H. V. Demir, "Vacuum-evaporated lead halide perovskite LEDs [Invited]," *Optical Materials Express*, vol. 12, no. 1, p. 256, 2022.

[6] F. Yan and H. V. Demir, "LEDs using halide perovskite nanocrystal emitters," *Nanoscale*, vol. 11, no. 24, pp. 11402–11412, 2019.

[7] D. Gets *et al.*, "Reconfigurable Perovskite LEC: Effects of Ionic Additives and Dual Function Devices," *Advanced Optical Materials*, vol. 9, no. 3, 2021.

[8] S. Akin, N. Arora, S. M. Zakeeruddin, M. Grätzel, R. H. Friend, and M. I. Dar, "New Strategies for Defect Passivation in High-Efficiency Perovskite Solar Cells," *Advanced Energy Materials*, vol. 10, no. 13, p. 1903090, Apr. 2020.

[9] L. Liu, K. Cao, S. Chen, and W. Huang, "Toward See-Through Optoelectronics: Transparent Light-Emitting Diodes and Solar Cells," *Advanced Optical Materials*, vol. 8, no. 22, pp. 1–31, 2020.

[10] Q. Dong, L. Lei, J. Mendes, and F. So, "Operational stability of perovskite light emitting diodes," *JPhys Materials*, vol. 3, no. 1, 2020.

[11] D. Vaufrey *et al.*, "ITO-on-top organic light-emitting devices: a correlated study of opto-electronic and structural characteristics," *Semiconductor Science and Technology*, vol. 18, no. 4, pp. 253–260, Apr. 2003.

[12] M. S. Miller, J. C. O'Kane, A. Niec, R. S. Carmichael, and T. B. Carmichael, "Silver nanowire/optical adhesive coatings as transparent electrodes for flexible electronics," *ACS Applied Materials and Interfaces*, vol. 5, no. 20, pp. 10165–10172, 2013.

[13] J. Liang, L. Li, X. Niu, Z. Yu, and Q. Pei, "Fully solution-based fabrication of flexible light-emitting device at ambient conditions," *Journal of Physical Chemistry C*, vol. 117, no. 32, pp. 16632–16639, 2013.

[14] Q. Wan *et al.*, "High-Efficiency Semitransparent Light-Emitting Diodes with Perovskite Nanocrystals," *ACS Applied Materials and Interfaces*, vol. 14, no. 17, pp. 19697–19703, 2022.

[15] L. Shi and Y. Cui, "High Performance Ultrathin MoO 3 / Ag Transparent Electrode and Its Application in Semitransparent Organic Solar Cells," 2018.

[16] Z. Yu *et al.*, "Fully bendable polymer light emitting devices with carbon nanotubes as cathode and anode," *Applied Physics Letters*, vol. 95, no. 20, pp. 2007–2010, 2009.

[17] N. Terasawa, K. Mukai, K. Yamato, and K. Asaka, "Superior performance of non-activated multi-walled carbon nanotube polymer actuator containing ruthenium oxide over a single-walled carbon nanotube," *Carbon*, vol. 50, no. 5, pp. 1888–1896, 2012.

[18] C. D. Williams, R. O. Robles, M. Zhang, S. Li, R. H. Baughman, and A. A. Zakhidov, "Multiwalled carbon nanotube sheets as transparent electrodes in high brightness organic light-emitting diodes," *Applied Physics Letters*, vol. 93, no. 18, pp. 2–5, 2008.

[19] P. Andričević *et al.*, "Light-Emitting Electrochemical Cells of Single Crystal Hybrid Halide Perovskite with Vertically Aligned Carbon Nanotubes Contacts," *ACS Photonics*, vol. 6, no. 4, pp. 967–975, 2019.

[20] M. Alahbakhshi *et al.*, "Bright perovskite light-emitting electrochemical cell utilizing

CNT sheets as a tunable charge injector," in *Organic and Hybrid Light Emitting Materials and Devices XXIV*, Aug. 2020, p. 55.

[21] C. Xie, X. Zhao, E. W. Y. Ong, and Z. K. Tan, "Transparent near-infrared perovskite light-emitting diodes," *Nature Communications*, vol. 11, no. 1, pp. 1–5, 2020.

[22] Y. Ding, B. He, J. Zhu, W. Zhang, G. Su, and J. Duan, "Advanced Modification of Perovskite Surfaces for Defect Passivation and Efficient Charge Extraction in Air-Stable CsPbBr 3 Perovskite Solar Cells," 2019.

[23] W. Shockley and W. T. Read, "Statistics of the recombinations of holes and electrons," *Physical Review*, vol. 87, no. 5, pp. 835–842, 1952.

[24] A. Mishra, M. Alahbakhshi, R. Haroldson, Q. Gu, A. A. Zakhidov, and J. D. Slinker, "Pure Blue Electroluminescence by Differentiated Ion Motion in a Single Layer Perovskite Device," vol. 2102006, pp. 1–9, 2021.

[25] N. Yantara *et al.*, "Inorganic Halide Perovskites for Efficient Light-Emitting Diodes," *Journal of Physical Chemistry Letters*, vol. 6, no. 21, pp. 4360–4364, 2015.

[26] T. Xu *et al.*, "Poly(ethylene oxide)-assisted energy funneling for efficient perovskite light emission," *Journal of Materials Chemistry C*, vol. 7, no. 27, pp. 8287–8293, 2019.

[27] J. Li, S. G. R. Bade, X. Shan, and Z. Yu, "Single-Layer Light-Emitting Diodes Using Organometal Halide Perovskite/Poly(ethylene oxide) Composite Thin Films," *Advanced Materials*, vol. 27, no. 35, pp. 5196–5202, 2015.

[28] A. Dutta, R. K. Behera, S. K. Dutta, S. Das Adhikari, and N. Pradhan, "Annealing CsPbX3 (X = Cl and Br) Perovskite Nanocrystals at High Reaction Temperatures: Phase Change and Its Prevention," vol. 3, 2018.

[29] M. Zhang *et al.*, "Growth and characterization of all-inorganic lead halide perovskite semiconductor CsPbBr3 single crystals," *CrystEngComm*, vol. 19, no. 45, pp. 6797–6803, 2017.

[30] B. K. Money and J. Swenson, "Dynamics of poly(ethylene oxide) around its melting temperature," *Macromolecules*, vol. 46, no. 17, pp. 6949–6954, 2013.

[31] M. Zhang *et al.*, "Strong, Transparent, Multifunctional, Carbon Nanotube Sheets," *Science*, vol. 309, no. 5738, pp. 1215–1219, Aug. 2005.

[32] K. Balasubramanian and M. Burghard, "Chemically functionalized carbon nanotubes," *Small*, vol. 1, no. 2, pp. 180–192, 2005.

[33] J. Liu *et al.*, "Fullerene pipes," *Science*, vol. 280, no. 5367, pp. 1253–1256, 1998.

[34] W. Xia, C. Jin, S. Kundu, and M. Muhler, "A highly efficient gas-phase route for the oxygen functionalization of carbon nanotubes based on nitric acid vapor," *Carbon*, vol.

47, no. 3, pp. 919–922, 2009.

[35] V. Datsyuk *et al.*, "Chemical oxidation of multiwalled carbon nanotubes," *Carbon*, vol. 46, no. 6, pp. 833–840, 2008.

[36] G. Zhang, S. Sun, D. Yang, J. P. Dodelet, and E. Sacher, "The surface analytical characterization of carbon fibers functionalized by H2SO4/HNO3 treatment," *Carbon*, vol. 46, no. 2, pp. 196–205, 2008.

[37] R. R. N. Marques, B. F. Machado, J. L. Faria, and A. M. T. Silva, "Controlled generation of oxygen functionalities on the surface of Single-Walled Carbon Nanotubes by HNO3 hydrothermal oxidation," *Carbon*, vol. 48, no. 5, pp. 1515–1523, 2010.

[38] A. Jorio, M. A. Pimenta, A. G. S. Filho, and R. Saito, "Characterizing carbon nanotube samples with resonance Raman scattering," *New Journal of Physics*, vol. 5, pp. 139–139, 2003.

[39] S. Osswald, M. Havel, and Y. Gogotsi, "Monitoring oxidation of multiwalled carbon nanotubes by Raman spectroscopy," *Journal of Raman Spectroscopy*, vol. 38, no. 6, pp. 728–736, Jun. 2007.

[40] T. Wang, K. Jeppson, and J. Liu, "Dry densification of carbon nanotube bundles," *Carbon*, vol. 48, no. 13, pp. 3795–3801, 2010.

[41] Y. D. Lim, Q. Kong, S. Wang, C. W. Tan, B. K. Tay, and S. Aditya, "Enhanced field emission properties of carbon nanotube films using densification technique," *Applied Surface Science*, vol. 477, pp. 211–219, 2019.

[42] Y. Wang *et al.*, "Tuning carbon nanotube assembly for flexible, strong and conductive films," *Nanoscale*, vol. 7, no. 7, pp. 3060–3066.

[43] S. Li *et al.*, "Enhancement of carbon nanotube fibres using different solvents and polymers," *Composites Science and Technology*, vol. 72, no. 12, pp. 1402–1407, 2012.

[44] M. A. Correa-Duarte, N. Wagner, J. Rojas-Chapana, C. Morsczeck, M. Thie, and M. Giersig, "Fabrication and Biocompatibility of Carbon Nanotube-Based 3D Networks as Scaffolds for Cell Seeding and Growth," *Nano Letters*, vol. 4, no. 11, pp. 2233–2236, Nov. 2004.

[45] D. Choquesillo-Lazarte and J. M. García-Ruiz, "Poly(ethylene) oxide for small-molecule crystal growth in gelled organic solvents," *Journal of Applied Crystallography*, vol. 44, no. 1, pp. 172–176, 2011.

[46] D. Costa, *Light-Emitting Electrochemical Cells*, vol. 1606392, no. 2017. Cham: Springer International Publishing, 2017.

[47] T. J. Simmons, J. Bult, D. P. Hashim, R. J. Linhardt, and P. M. Ajayan, "Noncovalent

Functionalization as an Alternative to Oxidative Acid Treatment of Single Wall Carbon Nanotubes with Applications for Polymer Composites," *ACS Nano*, vol. 3, no. 4, pp. 865–870, Apr. 2009.

[48] X. Xiao *et al.*, "Capacitance-voltage characteristics of perovskite light-emitting diodes: Modeling and implementing on the analysis of carrier behaviors," *Applied Physics Letters*, vol. 120, no. 24, 2022.

[49] W. Liu and G. Speranza, "Tuning the Oxygen Content of Reduced Graphene Oxide and Effects on Its Properties," *ACS Omega*, vol. 6, no. 9, pp. 6195–6205, 2021.

[50] E. Bodyago, D. Gets, M. Baeva, I. Mukhin, S. Makarov, and A. Zakhidov, "Multi wall carbon nanotubes as a top electrode for perovskite light-emitting electrochemical cells," *Journal of Physics: Conference Series*, vol. 2015, no. 1, 2021.

[51] T. Kirchartz, J. A. Márquez, M. Stolterfoht, and T. Unold, "Photoluminescence-Based Characterization of Halide Perovskites for Photovoltaics," *Advanced Energy Materials*, vol. 10, no. 26, p. 1904134, Jul. 2020.

[52] A. E. Goldt *et al.*, "Highly efficient bilateral doping of single-walled carbon nanotubes," *Journal of Materials Chemistry C*, vol. 9, no. 13, pp. 4514–4521, 2021.